Magnetism and heterogeneity of Co in anatase Co:TiO_2 magnetic semiconductor

Y. J. Lee, M. P. de Jong, and R. Jansen[a)]
MESA+ Institute for Nanotechnology, University of Twente, 7500 AE Enschede, The Netherlands

(Received 19 October 2009; accepted 30 January 2010; published online 24 February 2010)

Using x-ray magnetic circular dichroism (XMCD), x-ray absorption spectroscopy (XAS), and energy filtered transmission electron microscopy, we provide evidence for a heterogeneous Co distribution in anatase Co:TiO_2 magnetic semiconductor having a low Co concentration (1.4 at. %). Multiplet structure due to Co^{2+} is observed in XAS spectra, but suppressed due to the coexistence of metallic Co clusters and substitutional Co ions, whereas XMCD spectra resemble metallic Co. The presence of Co^{2+} can be correlated with earlier observations of impurity band conduction and Kondo behavior, whereas metallic Co clusters contribute to the ferromagnetism and anomalous Hall effect. © *2010 American Institute of Physics*. [doi:10.1063/1.3327805]

The prediction of magnetism in wide band gap oxides and nitrides[1] has triggered much interest in room temperature dilute magnetic semiconductors for practical spintronic devices. One of the most well-studied materials is the Co doped TiO_2 semiconductor for which room temperature ferromagnetism,[2] anomalous Hall effect (AHE),[3–6] magneto-optical dichroism,[7,8] and transport studies[9–12] have been reported. However, there is still controversy about the origin of the observed ferromagnetism and related effects, i.e., whether the ferromagnetism is induced by a carrier-mediated exchange interaction between substitutional magnetic ions, or by defects or extrinsic sources.[4,13–15]

In previous work, we observed ferromagnetism and AHE at room temperature in anatase Co:TiO_2 thin films grown under oxygen poor conditions.[6] In the same material, conduction in a metallic impurity band was demonstrated,[11] consistent with a mechanism of ferromagnetic exchange interaction between localized moments via this donor impurity band.[16] Evidence was also found for the Kondo effect due to the resonant interaction of conduction electrons with local Co magnetic moments.[11] However, the strong coupling between carriers and a local moment in the Kondo regime causes screening and no long range ferromagnetic order.[17] For weaker coupling ferromagnetic order can arise through a long range interaction mediated by polarized conduction electrons.[17] A combined observation of ferromagnetism and Kondo effect in Co:TiO_2 indicates a possible inhomogeneous distribution of Co.

To investigate this conjecture, we present a combined soft x-ray absorption spectroscopy (XAS), x-ray magnetic circular dichroism (XMCD), and energy filtered transmission electron microscopy (EF-TEM) study of anatase TiO_2 with a low Co concentration of 1.4 at. %. We examine films grown under oxygen rich (10^{-3} mbar) and oxygen poor (9×10^{-5} mbar) conditions having different magnetic properties at room temperature, i.e., paramagnetic and ferromagnetic, respectively. The XAS and XMCD data reveals the coexistence of ionic Co^{2+} and metallic Co in both type of films. The presence of Co heterogeneity was confirmed by EF-TEM.

Epitaxial thin films of anatase Co:TiO_2 (1.4 at. %) were grown by pulsed laser deposition on TiO_2-terminated $SrTiO_3$ substrates under oxygen rich (10^{-3} mbar, film thickness 45 nm) and oxygen poor (9×10^{-5} mbar, film thickness 10 nm) conditions. More details on growth, transport, and magnetic properties have been presented previously.[6,11] For comparison, a 2 nm thick reference Co metal thin film was fabricated with a capping layer of 3 nm thick Al. The XAS and XMCD measurements, both at the Co $L_{2,3}$ edge, were performed at beam line I1011 of MAX-laboratory in Lund, Sweden, which uses a circular polarized undulator, providing 60% left and right handed circular polarization. All spectra were measured at room temperature in total electron yield mode, with a probing depth of about 10 nm. The XMCD spectra were obtained at a fixed photon helicity and an angle of incidence of 45° with respect to the sample normal. To reverse the sample magnetization, an *in situ* magnetic field was applied colinear with the x-ray beam (for Co:TiO_2 samples) or in the film plane (Co metal reference sample).

The top panel of Fig. 1 shows XMCD spectra (blue lines) of oxygen rich (10^{-3} mbar) and oxygen poor films (9×10^{-5} mbar), obtained by subtracting XAS measurements (black and red) performed with circularly polarized light for opposite magnetization directions. The XMCD spectrum of the oxygen rich sample, which shows paramagnetism as concluded previously from magnetometry,[11] was measured under application of a small magnetic field (±0.08 T). The sample grown under oxygen poor conditions is ferromagnetic and was measured in remanence at zero magnetic field, after application of a ±0.5 T field. A clear XMCD signal is observed for both films. It is larger by about a factor of 1.7 for the oxygen poor film. Additional XMCD measurements were performed on a reference Co metal thin film, shown in the bottom panel together with the normalized XMCD data for the Co:TiO_2 films. Also shown is the simulated XMCD spectrum of Co^{2+} ions in CoO, obtained with the same parameters as described below for the simulated XAS spectrum. Strikingly, the XMCD spectra of both the Co:TiO_2 films are very similar to the featureless Co-metal spectrum, which suggests that the magnetic moments arise from the presence of metallic Co in the Co:TiO_2. However, it should be noted that the data does not allow us to conclude that *all* magnetic moments arise from metallic Co. The spec-

a)Electronic mail: ron.jansen@el.utwente.nl.

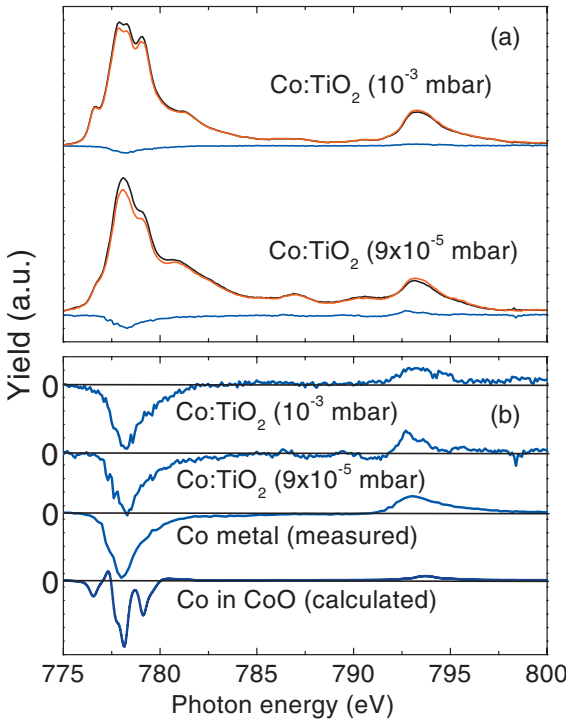

FIG. 1. (Color) (a) Two Co $L_{2,3}$ edge XAS spectra recorded with circularly polarized light of helicity anti-parallel (red line, I^-) and parallel (black line, I^+) to the magnetization, respectively, for a 45 nm $Co:TiO_2$ film grown at 10^{-3} mbar oxygen, and a 10 nm $Co:TiO_2$ film grown at 9×10^{-5} mbar oxygen. Also shown (in blue) is the resulting $L_{2,3}$ edge XMCD, obtained as the difference $(I^- - I^+)$. (b) Magnified $L_{2,3}$ edge XMCD, displayed together with the XMCD of a 2 nm thick reference Co metal film, and the simulated XMCD spectrum of Co^{2+} in CoO. The four spectra are normalized to obtain the same peak amplitude around 778 eV.

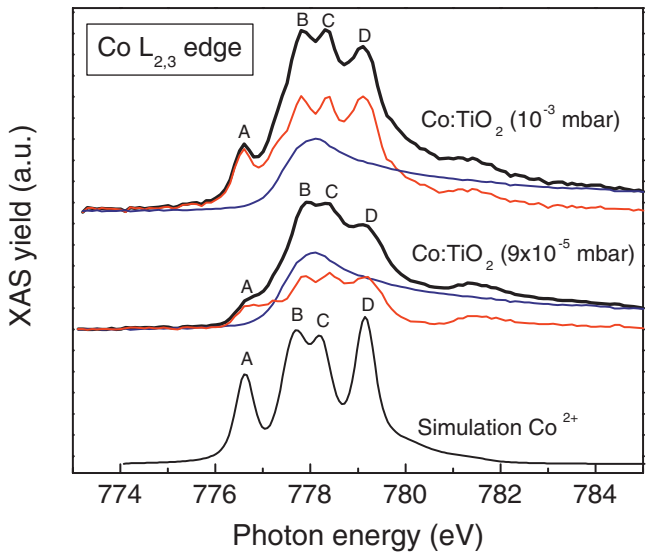

FIG. 2. (Color) Black lines: experimental XAS data of a 45 nm $Co:TiO_2$ film grown at 10^{-3} mbar oxygen, a 10 nm film grown at 9×10^{-5} mbar oxygen, and the simulated spectrum of Co^{2+} ions. Red lines: difference spectra with a much clearer fine structure obtained by subtraction of a weighted metallic Co contribution (blue lines) from the measured XAS spectra, as described in the text.

tra can, within the accuracy of the measurement, also be described reasonably by metallic Co plus a contribution to the magnetism from Co-ions of up to 30%. This would produce an XMCD spectrum with a weak multiplet structure that is hard to distinguish from the XMCD spectrum of pure Co metal.

Figure 2 shows Co $L_{2,3}$ edge XAS spectra obtained with linearly polarized x-rays. Also shown is a calculated spectrum for Co^{2+} ions, obtained by ligand field multiplet (LFM) calculations as developed by Thole and co-workers, based on Cowan's atomic multiplet code and Butler's group theoretical code.[18] The LFM calculation was performed for Co^{2+} ions $(3d^7)$ in a cubic crystal field (O_h symmetry) with $10Dq=1.1$ eV, corresponding to a high-spin state. The Hartree–Fock Slater integrals were scaled to 75% of their atomic values to account for solid state effects. The overall good agreement in the energy position of multiplet features (except for a small shift of the two central peaks B and C) between the calculated multiplet spectrum and the experimental spectra shows that both samples contain substitutional Co^{2+}. However, a distinct difference between the two XAS spectra is that the multiplet features are much more pronounced for the oxygen-rich grown $Co:TiO_2$ thin film. The spectrum with suppressed multiplet-related fine structure is quite similar to previously reported Co $L_{2,3}$ edge XAS data of rutile $Co:TiO_2$ thin films.[19]

The results described above show that the Co distribution is heterogeneous, consisting of metallic Co (as seen in XMCD) and ionic Co^{2+} (as seen in XAS). This suggests that the suppressed XAS multiplet structure is related to a superimposed featureless Co metal contribution. To test this, we subtracted weighted Co-metal spectra (blue lines in Fig. 2) obtained from the Co-metal reference sample. The difference spectra after subtraction (red lines in Fig. 2) represent the Co^{2+} contributions, and indeed show a more pronounced multiplet structure. The weight of the subtracted Co-metal contribution was taken such that, for both samples, the multiplet features labeled B, C, and D, are all at about the same height in the difference spectra. Using this criterion, the difference curves closely mimic the spectral shape of CoO, which contains Co^{2+} in an octahedral crystal field of essentially the same strength $(1.05\pm0.05$ eV).[20] The weights of the metallic Co contribution to the total XAS intensity amount to 60% and 40% (in terms of peak heights) for the $Co:TiO_2$ films grown under oxygen poor and oxygen rich conditions, respectively. The stronger suppression of the Co^{2+} multiplet structure for the oxygen-poor grown $Co:TiO_2$ sample is thus consistent with the presence of a larger amount of metallic Co. After the Co metal contribution is subtracted, the multiplet features (red lines) are not exactly the same for the two samples. There is some additional broadening of the multiplet structure for the oxygen-poor grown film that cannot be explained by the presence of a metallic Co contribution. This broadening can be due to variations in the local crystal fields, perhaps due to oxygen vacancies, or some finite contribution of magnetic coupling via conduction electrons, for which the XAS spectrum of $Co:TiO_2$ is not known.

We performed complementary EF-TEM measurements, which uses specific energy loss peaks of the transmitted electrons to obtain spatial maps of the concentration of a particular chemical element. Both oxygen rich and oxygen poor $Co:TiO_2$ samples were studied. Finding the Co metal clusters is by no means an easy task, especially for the paramagnetic oxygen-rich grown $Co:TiO_2$ thin film, considering that the superparamagnetic Co particle size is below 10 nm. Not-

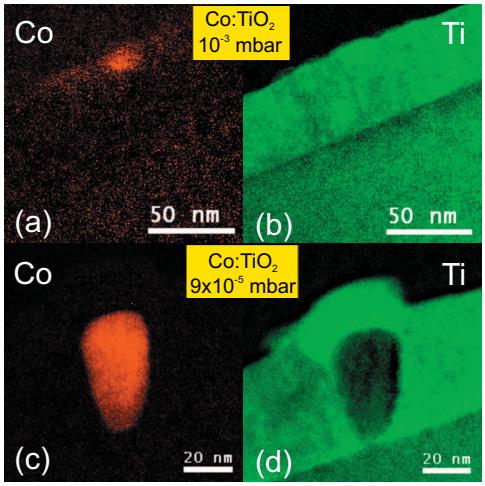

FIG. 3. (Color) EF-TEM images of a 45 nm $Co:TiO_2$ film grown at 10^{-3} mbar oxygen [(a) and (b)] and a 45 nm $Co:TiO_2$ film grown at 9×10^{-5} mbar oxygen [(c) and (d)]. Images (a) and (c) represent maps of the concentration of elemental Co (in red), while (b) and (d) are maps for Ti (in green).

withstanding, for the $Co:TiO_2$ thin film grown under oxygen rich conditions, tiny regions of enhanced Co concentration near the surface were observed [Fig. 3(a)]. In contrast, for the $Co:TiO_2$ thin film grown under oxygen poor conditions, relatively large Co-rich clusters emanating from the substrate/film interface and spanning the full film thickness [Fig. 3(c)] were easily spotted using EF-TEM. These findings confirm the conclusions from the x-ray measurements that the Co distribution is inhomogeneous.

The Co distribution is heterogeneous for $Co:TiO_2$ films grown under oxygen rich as well as oxygen poor conditions, and more so for the latter. The presence of substitutional Co^{2+} can be correlated with the earlier observation of impurity band conduction and Kondo behavior,[11] whereas metallic Co contributes to the ferromagnetism and AHE.[6] Based on the XAS spectra, approximately half of the 1.4% Co is metallic. Assuming a magnetic moment of 1.7 Bohr magneton per Co metal atom, the corresponding magnetization is 3.2 kA/m. This is consistent with the previously measured[6,11] remanent magnetization of 2 to 4 kA/m, but smaller than the saturation magnetization (6–8 kA/m). However, the magnetometry data was obtained on thicker films (200 nm). Also, the fraction of metallic Co content derived from the XAS spectra refers to the XAS signal amplitude. Converting this to an atomic fraction needs to take the probing depth and a possible inhomogeneous depth profile of the metal/ion ratio into account. We stress that the XMCD data do not rule out a finite contribution of magnetism from ionic Co. Hence, our data, while suggestive of an extrinsic origin, does not establish the complete *absence* of ferromagnetism and AHE arising from the coupling of Co^{2+} ions by the conduction electrons.

This work was financially supported by the Netherlands Nanotechnology Network NANONED (supported by the Ministry of Economic Affairs).

[1] T. Dietl, H. Ohno, F. Matsukura, J. Cibert, and D. Ferrand, Science **287**, 1019 (2000).
[2] Y. Matsumoto, M. Murakami, T. Shono, T. Hasegawa, T. Fukumura, M. Kawasaki, P. Ahmet, T. Chikyow, S. Koshihara, and H. Koinuma, Science **291**, 854 (2001).
[3] H. Toyosaki, T. Fukumura, Y. Yamada, K. Nakajima, T. Chikyow, T. Hasegawa, H. Koinuma, and M. Kawasaki, Nature Mater. **3**, 221 (2004).
[4] S. R. Shinde, S. B. Ogale, J. S. Higgins, H. Zheng, A. J. Millis, V. N. Kulkarni, R. Ramesh, R. L. Greene, and T. Venkatesan, Phys. Rev. Lett. **92**, 166601 (2004).
[5] K. Ueno, T. Fukumura, H. Toyosaki, M. Nakano, and M. Kawasaki, Appl. Phys. Lett. **90**, 072103 (2007).
[6] R. Ramaneti, J. C. Lodder, and R. Jansen, Appl. Phys. Lett. **91**, 012502 (2007).
[7] H. Toyosaki, T. Fukumura, Y. Yamada, and M. Kawasaki, Appl. Phys. Lett. **86**, 182503 (2005).
[8] Y. Hirose, T. Hitosugi, Y. Furubayashi, G. Kinoda, K. Inaba, T. Shimada, and T. Hasegawa, Appl. Phys. Lett. **88**, 252508 (2006).
[9] R. J. Kennedy, P. A. Stampe, E. Hu, P. Xiong, S. von Molnar, and Y. Xin, Appl. Phys. Lett. **84**, 2832 (2004).
[10] H. Toyosaki, T. Fukumura, K. Ueno, M. Nakano, and M. Kawasaki, Jpn. J. Appl. Phys., Part 2 **44**, L896 (2005).
[11] R. Ramaneti, J. C. Lodder, and R. Jansen, Phys. Rev. B **76**, 195207 (2007).
[12] E. Hu, S. von Molnar, P. A. Stampe, R. J. Kennedy, and Y. Xin, Appl. Phys. Lett. **92**, 012114 (2008).
[13] J.-Y. Kim, J.-H. Park, B.-G. Park, H.-J. Noh, S.-J. Noh, J. S. Yang, D.-H. Kim, S. D. Bu, T.-W. Noh, H.-J. Lin, H.-H. Hsieh, and C. T. Chen, Phys. Rev. Lett. **90**, 017401 (2003).
[14] T. C. Kaspar, S. M. Heald, C. M. Wang, J. D. Bryan, T. Droubay, V. Shutthanandan, S. Thevuthasan, D. E. McCready, A. J. Kellock, D. R. Gamelin, and S. A. Chambers, Phys. Rev. Lett. **95**, 217203 (2005).
[15] S. A. Chambers, Surf. Sci. Rep. **61**, 345 (2006).
[16] J. M. D. Coey, M. Venkatesan, and C. B. Fitzgerald, Nature Mater. **4**, 173 (2005).
[17] T. Jungwirth, J. Sinova, J. Masek, J. Kucera, and A. H. MacDonald, Rev. Mod. Phys. **78**, 809 (2006).
[18] R. D. Cowan, *The Theory of the Atomic Structure and Spectra* (University of California Press, Berkley, 1981); P. H. Butler, *Point Group Symmetry Applications: Methods and Tables* (Plenum, New York, 1981).
[19] K. Mamiya, T. Koide, A. Fujimori, H. Tokano, H. Manaka, A. Tanaka, H. Toyosaki, T. Fukumura, and M. Kawasaki, Appl. Phys. Lett. **89**, 062506 (2006).
[20] F. M. F. de Groot, M. Abbate, J. van Elp, G. A. Sawatzky, Y. J. Ma, C. T. Chen, and F. Sette, J. Phys.: Condens. Matter **5**, 2277 (1993).